AMBIO 2014, 43:878–890
DOI 10.1007/s13280-013-0487-2

KUNGL. VETENSKAPS-AKADEMIEN
THE ROYAL SWEDISH ACADEMY OF SCIENCES

REPORT

Linking Cellulose Fiber Sediment Methyl Mercury Levels to Organic Matter Decay and Major Element Composition

Olof Regnell, Mark Elert, Lars Olof Höglund, Anna Helena Falk, Anders Svensson

Received: 27 June 2013 / Revised: 25 September 2013 / Accepted: 16 December 2013 / Published online: 14 January 2014

Abstract Methylation of mercury (Hg) to highly toxic methyl Hg (MeHg), a process known to occur when organic matter (OM) decomposition leads to anoxia, is considered a worldwide threat to aquatic ecosystems and human health. We measured temporal and spatial variations in sediment MeHg, total Hg (THg), and major elements in a freshwater lagoon in Sweden polluted with Hg-laden cellulose fibers. Fiber decomposition, confined to a narrow surface layer, resulted in loss of carbon (C), uptake of nitrogen (N), phosphorus (P), and sulfur (S), and increased MeHg levels. Notably, fiber decomposition and subsequent erosion of fiber residues will cause buried contaminants to gradually come closer to the sediment–water interface. At an adjacent site where decomposed fiber accumulated, there was a gain in C and a loss of S when MeHg increased. As evidenced by correlation patterns and vertical chemical profiles, reduced S may have fueled C-fixation and Hg methylation at this site.

Keywords Mercury · Methylation · Cellulose fiber · Decomposition · Major element cycles

INTRODUCTION

The elevated presence of Hg in the environment is a problem of global magnitude. Hg is highly toxic, especially in the form of MeHg, and has a strong tendency to escape to the atmosphere, from where it may be deposited on land and water surfaces far from its point of release. Because of bans on Hg use in industrial processes and products, many of the heavy Hg polluters stopped releasing Hg, but what they once released may constitute a serious local or even regional problem.

The forest industry and their associated chlor-alkali facilities have released large amounts of Hg to water, land, and air (e.g., Naturvårdsverket 1995; Sunderland and Chmura 2000). It has been estimated that the Swedish forest industry has released 1000 metric tons of Hg until 1994. Chlor-alkali plants were the main source, but as much as 145 tons of phenyl mercury acetate (PMA), a slimicide, may have been used by the pulp and paper industry to prevent fiber degradation between the early 40s and mid 60s (Naturvårdsverket 1995). Slimicides containing Hg were used in Canada and the US during approximately the same time period (Sunderland and Chmura 2000).

The present yearly emission of Hg to the atmosphere from Swedish sources is 500–700 kg according to the most recent estimates (Travnikov et al. 2012). Swedish Hg release directly to water is probably of the same order or less. The yearly wet deposition of Hg over Sweden is 1–3 tons, based on figures given by Travnikov et al. (2012). These figures are small in comparison with the amounts of Hg previously released by the Swedish forest industry and illustrate the importance of knowing the fate of legacy Hg in Sweden.

In addition to being a significant secondary Hg emission source, Hg released by forest industries is of particular concern because of its co-presence with large amounts of organic matter (OM). Notably, when OM decomposition leads to anaerobic microbial activity, Hg can be converted to highly toxic and bioavailable MeHg. The ability to methylate Hg is widespread among microorganisms in anoxic environments and has been demonstrated for sulfate-reducing bacteria (SRB) (e.g., Compeau and Bartha 1985), iron-reducing bacteria (FeRB) (e.g., Fleming et al. 2006), *Clostridia* (Pan-Hou and Imura 1982; Parks et al. 2013), and methanogens (Yu et al. 2013). When MeHg enters well-mixed water layers, it is taken up rapidly by

© Royal Swedish Academy of Sciences 2014
www.kva.se/en

phytoplankton and is further enriched at each trophic transfer (Watras and Bloom 1992). In most fish, virtually all Hg is in the form of MeHg (e.g., Bloom 1992), underscoring the role of Hg methylation in the accumulation of Hg by the aquatic biota.

Given the large number of waters affected by Hg and OM released by the forest industry, surprisingly little is known about the biogeochemistry of Hg and OM in these waters. In risk assessment of Hg-laden cellulose fiber sediment, it is vital to know the processes driving fiber decomposition, because the fate of Hg is strongly affected by microbial activities associated with fiber decomposition and by the extent to which fibers are decomposed. Any change in environmental conditions leading to increased fiber decomposition is likely to increase Hg exposure of fish and other organisms in fiber-polluted waters.

In order to identify the processes driving fiber decomposition, we measured spatial and temporal changes in sediment major element composition. Simultaneous measurements of sediment THg and MeHg levels made it possible to infer how the various biogeochemical processes involved in fiber decomposition affected Hg methylation and Hg retention. We made our measurements in fiber sediment in a freshwater lagoon that has received effluents from a paper mill. The study highlights processes and conditions that affect fiber decomposition, Hg mobility, and Hg speciation.

MATERIALS AND METHODS

Study Site

We conducted our study in the inner basin of a freshwater lagoon, Nötöfjärden, southeast Sweden, separated from the Baltic Sea by an overflow weir in the narrow passage between two peninsulas (Fig. 1). The area of the entire lagoon is 0.58 km^2 and the mean water depth 1.7 m. The inner basin is polluted with cellulose fiber (mostly from sulfite pulp) that was released into its feeding stream by a paper mill. The present Hg content of the cellulose fiber sediment has been estimated to 25 kg (IVL, unpublished results). The pulp was treated with Hg, probably PMA, until the use of Hg as a biocide was prohibited (mid 60s). Given the low stability of phenyl mercury (Gavis and Ferguson 1972), most of the Hg is probably inorganic in the bioactive layers, but this has not been confirmed by measurements.

The sampling sites F1 and F2 were shallow sites (water depths: 1.2 and 2.1 m, respectively) well within the fiber sediment area, whereas A1 (water depth: 3.1) was located at the maximum water depth of the lagoon (Fig. 1). Based on the earlier studies of the fiber sediment topography and water depths of the lagoon (Hultgren 2000), we assumed that A1 was a site at which fine-particulate matter accumulated, and F1 and F2 sites at which no or little accumulation occurred. Indeed, these assumptions were confirmed by ocular inspection of sediment cores showing only a thin layer of detritus on top of fibers of variable decomposition states at F1 and F2, and a substantial detritus layer at A1. The element analyses (C:N ratios) confirmed that more or less intact fibers were present close to the sediment surface at F1 and F2, but not at A1 (see "Result" section).

Sampling

Sediment samples from the sites F1, F2, and A1 were collected at approximately monthly intervals (12 times) between November 6, 2003 and October 6, 2004. On each occasion and from each site, five sediment samples were taken from the 0–1 cm and the 1–5 cm sediment layers, respectively, except that only three sediment samples were taken in January from A1. Also, in a few cases, there was not enough sediment for the analysis of Fe, P, and S in the 0–1 cm layer (14 samples altogether). The rationale behind sampling both the 0–1 cm and the 1–5 cm layers was to be able to judge the extent to which settling matter and mixing were responsible for changes seen in these layers.

On May 17, longer cores were extracted (0–100 cm), one at each station, and divided into 1-, 2-, 5-, and 10-cm slices depending on depth. However, the integrity of the upper 0–10 cm layers was not satisfactory so we re-sampled the 0–10 cm layers on June 3.

Two different types of sediment samplers were used to collect samples from the 0–1 cm and 1–5 cm sediment layers. They both performed well if operated properly. One type consisted of a plastic tube (Ø: 50 mm) that was attached to a rod (KC model A, Swedaq). The other was of Benell type (Swedaq) and consisted of a plastic tube (Ø: 70 mm) that was inserted into a weighted holder and operated with a line. Keeping the lower end of the tube below the water surface, a piston was inserted into the tube that was used to push the sediment core upwards into the slicing device placed on top of the tube.

To obtain the long cores (0–100 cm), another sediment sampler (von Post–Wik) was used. It consists of a 2-m plastic tube (Ø: 40 mm) equipped with a tight fitting piston on a rod of the same length as the plastic tube, the rod in turn being attached to a line held by the operator. The plastic tube, initially being held just above the sediment surface, is pressed into the sediment with the aid of connectable aluminum tubes while keeping the piston in the same position above the sediment surface. After evacuating the water above the sediment by turning the piston and pressing it toward the sediment surface, the sediment core is pushed out of the tube into a slot with cm marks with a

© Royal Swedish Academy of Sciences 2014

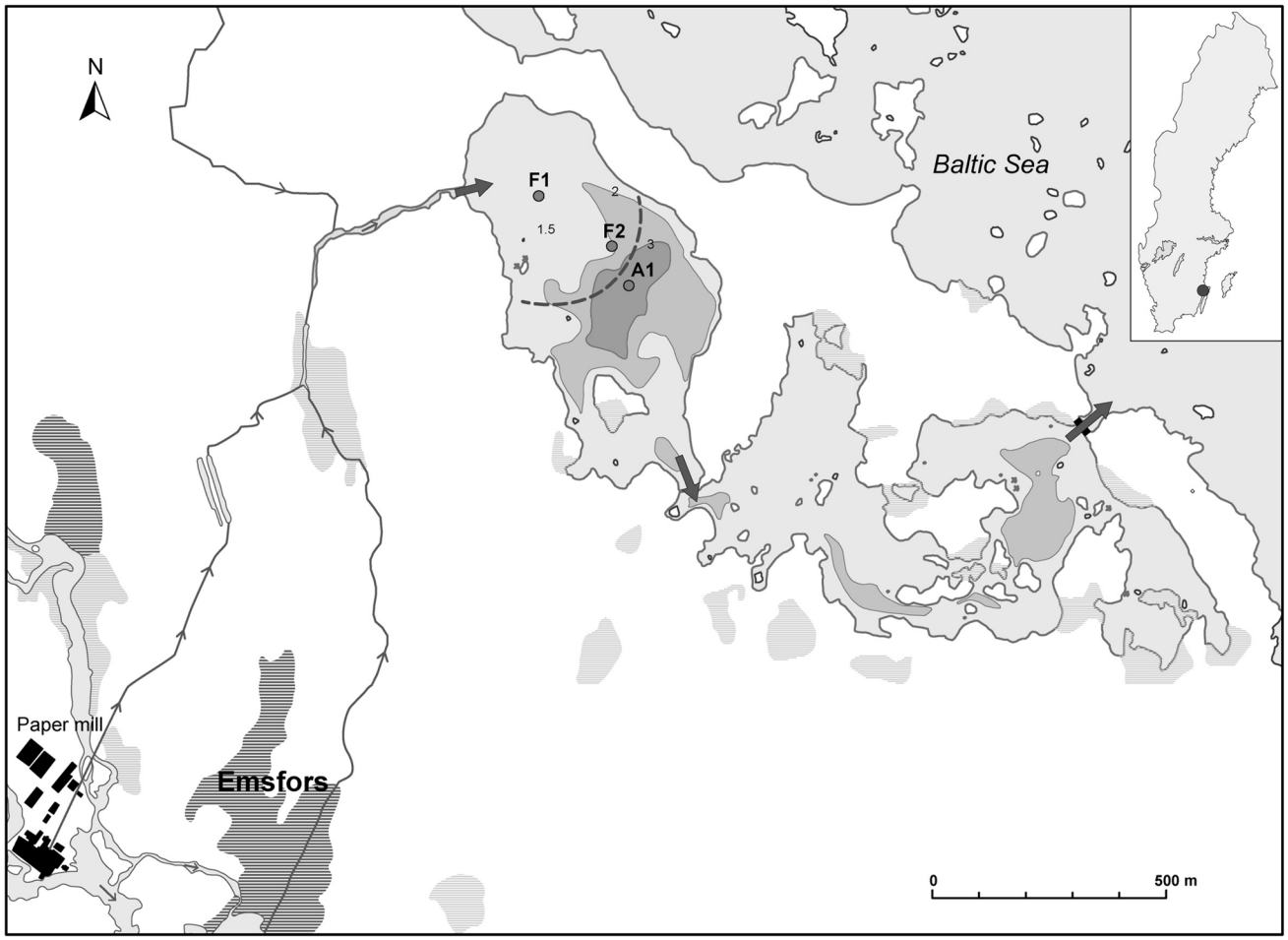

Fig. 1 The freshwater lagoon with the sampling sites F1, F2, and A1, and the location of the historical source of pollution (paper mill). The *broken line* shows the approximate border between fiber sediment with only a thin detritus layer on top of more or less intact cellulose fibers (*upper left*) and sediment with a substantial upper detritus layer (*lower right*). *Arrows* show the direction of water flow. The *inset* map shows the location in Sweden

minimum of compression. However, low stability of the upper parts of the long cores forced us to re-sample the 0–10 cm layers using the Benell type sampler.

Chemical Analyses

For THg determination, sediment was wet oxidized with H_2SO_4/HNO_3. The sample was subjected to refluxing by heating on a hot plate for about 6 h. To ensure complete oxidation, BrCl was then added. After dilution with MQ water, the resulting solution was analyzed for THg by a double-amalgamation method and CVAFS detection. The detection limit was on average 0.06 ng Hg g dw^{-1}.

MeHg was extracted from sediment by distillation by adding KCl and H_2SO_4 and heating. The MeHg was then ethylated in the aqueous phase by adding $NaB(C_2H_5)_4$, purged from solution using nitrogen gas, and collected onto Tenax^{TM} traps. The ethylated methyl mercury was thermally desorbed from the trap and carried on argon through a chromatographic column and separated isothermally from other Hg compounds. When reaching the pyrolysis unit, it was converted to gaseous Hg^0 and quantified by CVFAS. The detection limit for MeHg was on average 0.06 ng Hg g dw^{-1}.

Standard reference material (estuarine sediment, IAEA 405) was included in all sample runs. For THg, the measured values were all within −2.8 to 4.9 % of the certified value (0.81 μg Hg g dw^{-1}) and for MeHg within ±10 % of the certified value (0.00549 μg Hg g dw^{-1}).

Total C (TC) was determined using a carbon analyzer (Method: EN-13137, thermal oxidation, and infrared detection). Loss on ignition (LOI) was determined by combustion of dried sediment for 2 h at 550 °C, the first step being drying the sediment at 105 °C until constant weight was obtained. Total N (TN) was measured as Total Kjeldahl Nitrogen (Method: SNV 3674).

The elements Fe, P, and S were extracted from dried sediment samples (dried at 50 °C) in closed Teflon

© Royal Swedish Academy of Sciences 2014
www.kva.se/en

containers with 7 M HNO_3. After heating in a microwave oven for about 30 min at maximum pressure, the liquid phase was diluted to approximately 1.4 M HNO_3. The elements were quantified using an ICP-AES instrument according to EPA 200.7.

The results were dry weight corrected based on % dry weight determination of sub-samples (dried at 105 °C until constant weight).

Data Analysis

Relationships between variables were investigated performing simple, multiple, and forward stepwise multiple regressions. Concentrations were log-transformed prior to regression analyses unless otherwise stated. Notably, log-transformed and untransformed concentrations resulted in similar regressions and significance probabilities. A critical significance level of $p = 0.05$ was chosen. All data were included in the calculations, except for a few having values that were considered outliers, either based on deviation from the mean (>3 SD), or in the case of two LOI values based on simultaneously measured TC values, of which the former but not the latter showed large deviation from the mean. All together, three LOI and five values of each of total S (TS), total P (TP), and total Fe (TFe) were excluded from the calculations. The TS, TP, and TFe outliers were probably correctly measured but were atypically high.

RESULTS

Stratigraphy

The long cores (0–100 cm) from the fiber deposit at F1 and F2 showed variable THg concentration with depth. At both stations, THg in the 0–10 cm layer varied between 1 and 3 μg Hg g dw^{-1}. Two maxima were present at greater sediment depths. MeHg increased rapidly toward the surface in the 0–10 cm layer in both cores. Below this layer, MeHg was invariably low. TS, TP, TFe, and TN also displayed increasing concentration toward the sediment surface, whereas TC showed the opposite trend (Fig. 2). Consequently, MeHg was negatively correlated with TC and LOI, and positively correlated with TN, TP, and TS in the 0–10 cm sediment layer (Table 1). The enrichment of N, P, and S was not mainly an effect of mass loss resulting from OM mineralization (Fig. 3).

In the core from A1, the vertical concentration profiles were entirely different from those from F1 and F2, except for the sharp increase in MeHg toward the sediment surface. There was a buried MeHg peak not seen in the F1 and F2 cores. It coincided with peak values of TS, TP, TFe, and TC. THg displayed a maximum at a sediment depth between 60 and 70 cm. In the sediment above this depth, THg increased steadily toward the surface (Fig. 2). As opposed to the cores from F1 and F2, MeHg was positively instead of negatively correlated with LOI in the 0–10 cm layer. Neither TFe nor TS was significantly correlated with MeHg, but there was a strong positive correlation between MeHg and the TFe:TS ratio (Table 1). The TC and TN levels were relatively stable in the upper 0.5 m of the A1 core and similar to those of the surface layers at F1 and F2 (Fig. 2).

Temporal Study of the 0–1 cm and 1–5 cm Sediment Layers

At all stations, mean THg, whether log-transformed or not, tended to increase over time in the 1–5 cm layers, but significantly ($n = 12$, $p < 0.005$) only at A1 (Fig. 4). In the 0–1 cm layers, the tendency was the opposite, with a significant decrease in THg over time at F2 ($p < 0.05$). A relatively high loss of Hg from the 0–1 cm layer at F2 could be related to the fact that F2 showed the highest MeHg levels ($p < 0.0001$, ANOVA) (Fig. 4). MeHg is known to be more mobile than inorganic Hg (e.g., Regnell and Hammar 2004). Also, Hg methylation is associated with microbial activity that is likely to increase Hg mobilization (both inorganic Hg and MeHg) because of formation of Hg-sulfide complexes and decomposition of OM (Benoit et al. 1998).

MeHg increased over time at all stations and in both the 0–1 cm and the 1–5 cm layers (Fig. 4). There was a simultaneous decline in TC (and in LOI) at F1 and F2, suggesting that Hg was methylated in conjunction with OM mineralization. At A1, there was no decrease in TC, suggesting that Hg methylation was not strongly coupled to bulk OM mineralization.

During the rise in MeHg levels between May and June, there was a ≈4 °C increase in T above the sediment surface (from 10.5–12.9 to 13.9–17.1 °C), but there was an even steeper increase in T before May that did not result in clearly increasing MeHg levels, or in a clear decrease in TC levels at F1 and F2 (Figs. 4, 5). The spatial variation in TC at F1 and F2 was much larger before than after the June sampling, the opposite being true for the MeHg levels (Fig. 4).

The C:N ratios at F1 and F2 displayed a very clear difference in variation between the period before and that after the June sampling (Fig. 5). Apparently, there was very little available organic C left when the C:N ratio had dropped to around 30 mol mol^{-1}, preventing a further decrease in this ratio. Interestingly, the highest MeHg levels were found when the C:N ratio had dropped to this value. At A1, high MeHg levels occurred at C:N ratios

© Royal Swedish Academy of Sciences 2014

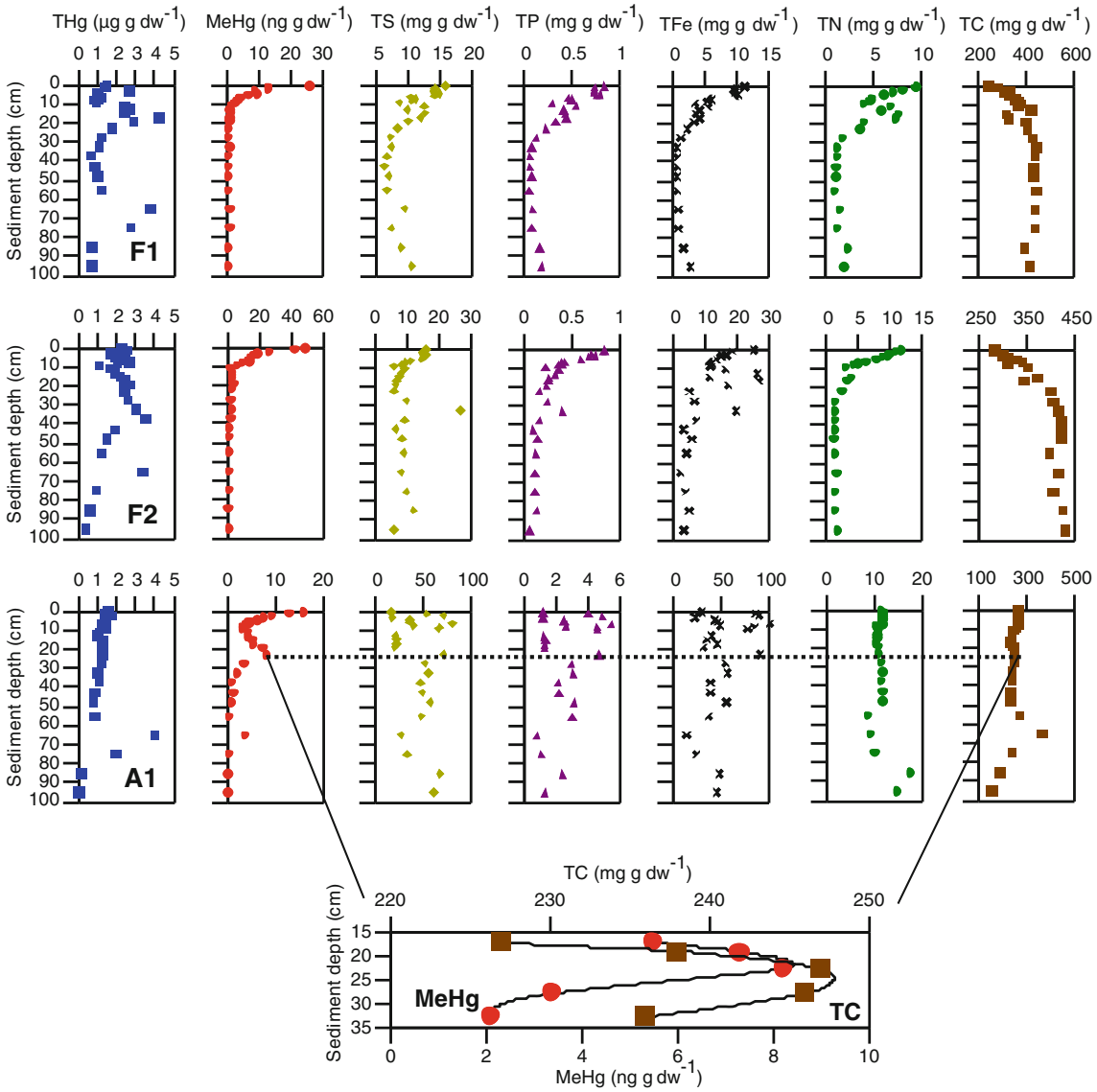

Fig. 2 Vertical concentration profiles of indicated sediment constituents at F1 (fiber sediment), F2 (fiber sediment), and A1 (nearby accumulation site). The *upper part* of the cores (0–10 cm) were taken on June 3, 2004, and the *lower part* (10–100 cm) on May 17, 2004. The *dashed line* shows the depth at which there was a local MeHg maximum at A1. The panel at the *bottom* shows the buried MeHg peak and the buried TC peak in magnification

Table 1 Correlation coefficient (r) for logMeHg versus log(indicated variable) in the 0–10 cm sediment layer with a vertical resolution of 1 cm ($n = 10$)

Station	TC	LOI	TN	TP	TS	TFe	TFe:TS	THg
F1	−0.90*	−0.98*	0.96*	0.88*	0.91*	0.88*	0.13	0.56
F2	−0.86*	−0.73*	0.91*	0.90*	0.82*	0.89*	−0.21	0.58
A1	0.69*	0.94*	0.58	−0.46	−0.49	−0.34	0.81*	0.42

* $p < 0.05$

similar to those at F1 and F2. Plotting MeHg against TS, it appears that MeHg at all stations increased with TS until a certain TS level was reached, and then decreased with increasing TS (Fig. 5).

TN, TP, and TS increased when TC decreased at F1 and F2 (Fig. 4). As for the vertical variation (Fig. 3), the increase of TN, TP, and TS between the May and the June sampling could not be explained more than to a minor

© Royal Swedish Academy of Sciences 2014
www.kva.se/en

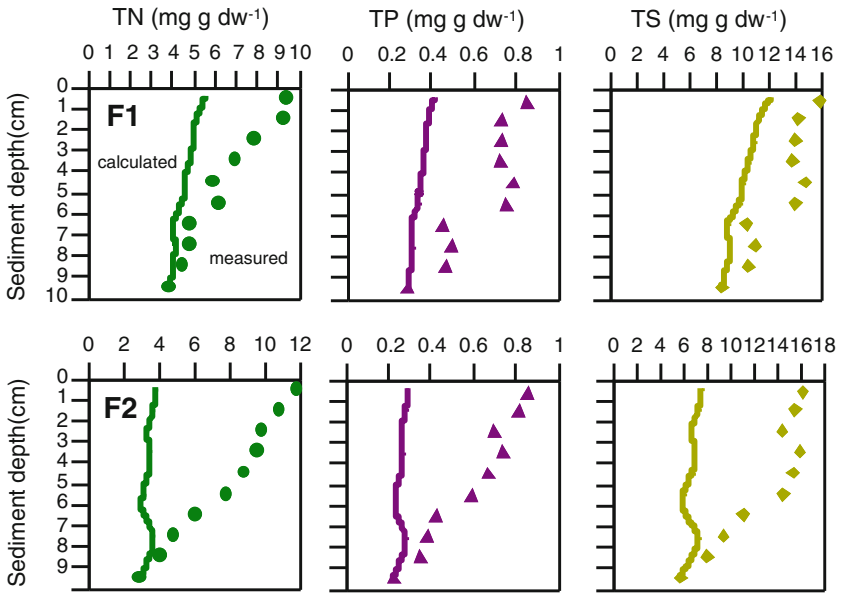

Fig. 3 The *symbols* show total N, total P, and total S levels, respectively, in the *upper* 10 cm of the long sediment cores from F1 and F2 (both fiber sediment). *Drawn lines* show what the levels would be if no uptake or release of N, P, and S had occurred and increasing matrix losses was the sole reason for increasing levels toward the sediment–water interface. Matrix loss was calculated from the change in loss on ignition (LOI) in relation to the LOI value at 10 cm

extent by matrix mass loss caused by OM mineralization (calculations not shown). At A1, there were no dramatic changes in major element composition during the study period (Fig. 4).

The correlation patterns displayed by MeHg in the 0–1 cm and 1–5 cm layers were consistent with those in the 0–10 cm layers of the long sediment cores (Tables 1, 2). We chose to present partial correlation coefficients for which time was held constant, because we considered similar or opposite change over time, e.g., gradual buildup or decay, without any direct causal relationship—a major confounding factor. Generally, holding time constant resulted in decreased correlation between MeHg and the ancillary sediment constituents (data not shown).

DISCUSSION

Vertical and Temporal Changes in Major Element Composition of Fiber Sediment

In undisturbed aquatic environments, labile C in settling matter is typically almost completely mineralized before being buried in zones of low biological activity. In contrast, the settling of cellulose fibers released by pulp and paper industries was so rapid and intense that labile C ended up in zones of low biological activity without being mineralized. Slow postdepositional mineralization of cellulose fibers is partly explained by the fact that efficient utilization of C-rich but nutrient-poor OM by microorganisms requires uptake of inorganic nutrients from other sources (Elser et al. 2000; Cleveland and Liptzin 2007).

In the long cores from F1 and F2, N, P, S, and Fe showed increasing enrichment while C showed increasing depletion from a sediment depth of about 30 cm toward the sediment–water interface (Fig. 2), suggesting that fiber decomposition was confined to the upper 30 cm of the fiber sediment. Alternatively, settling matter, e.g., algae, had shaped the major element profiles by simply diluting more or less intact fibers. The strongest argument against the latter interpretation is that N and P increased more and C decreased more in the 1–5 cm layers than in the 0–1 cm layers during the study period (Fig. 4). If settling matter was the cause of changing element levels, these changes should have been greater in the 0–1 cm layers than in the 1–5 cm layers, simply because the upper layer would be more affected by settling matter, and because any changes caused by settling matter would be four times more diluted in the 1–5 cm layers than in the 0–1 cm layers. Furthermore, when plotting the absolute changes in C, N, and P against the initial C, N, and P level, respectively, it can be seen that the absolute decrease in C increased with initial C level and that the absolute increase in N and P decreased with initial N and P level (Fig. 6). It is highly unlikely that such relationships should arise from dilution of fiber sediment by settling matter. Instead, these relationships suggest that assimilations of waterborne N and P by microbial cells were controlled by N and P requirements, and that a

© Royal Swedish Academy of Sciences 2014

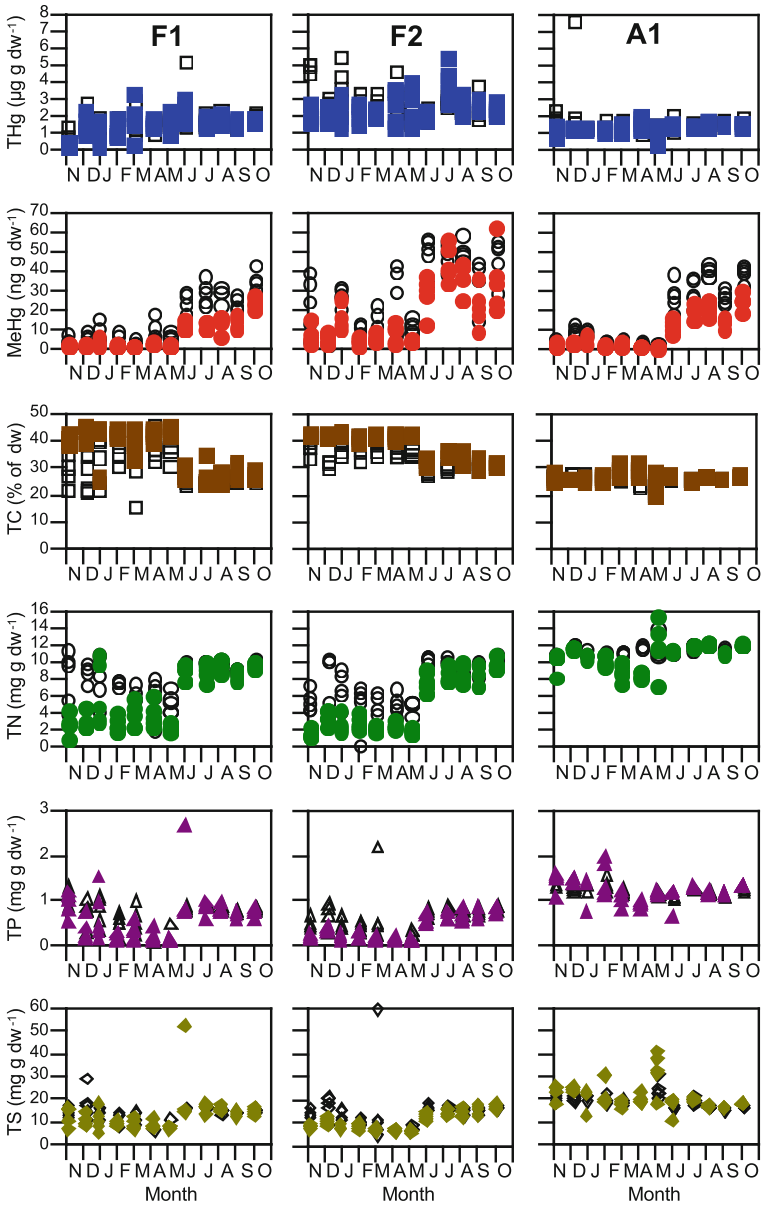

Fig. 4 Temporal changes in the 0–1 cm sediment layer (*open symbols*) and in the 1–5 cm sediment layer (*solid symbols*) during the study period November 6, 2003–October 6, 2004 of indicated variables at F1 (fiber sediment), F2 (fiber sediment), and A1 (nearby accumulation site). Results from all individual samples are shown in the plot, except for a few outlier TP and TS values off scale

high initial C level was indicative of a high fraction of easily available (labile) organic C, a fraction that decreased and finally was depleted during mineralization. Strong coupling between C mineralization, N and P assimilation, and SR could explain the fact that S displayed much the same relationship as N and P. Yet, it cannot be excluded that settling of algae or other labile OM components stimulated the decomposition of cellulose fibers. It is a well-known phenomenon that additions of labile OM can result in increased mineralization of more refractory OM (e.g., Fontaine et al. 2007).

In other words, the changes in the sediment at F1 and F2 were a result of the sediment stoichiometry approaching that of microbial cells until organic C was no longer available to fuel uptake of N and P, and SR. A simple physical mixing of the sediment would not result in an overall decrease in C and an overall increase in N and P (Fig. 6). A mixing extending deeper than 5 cm would have increased the C levels and decreased the N and P levels in the 0–1 and the 1–5 cm layers. Notably, the upper parts of the vertical depth profiles at F1 and F2 in Fig. 2 would have looked differently if a major physical mixing event had occurred. Furthermore, we deem it unlikely that settling of new matter on top of the cellulose fibers (algae, particulate matter imported by the stream) had a strong effect on these profiles, considering the fact that F1 and F2 were shallow

© Royal Swedish Academy of Sciences 2014
www.kva.se/en

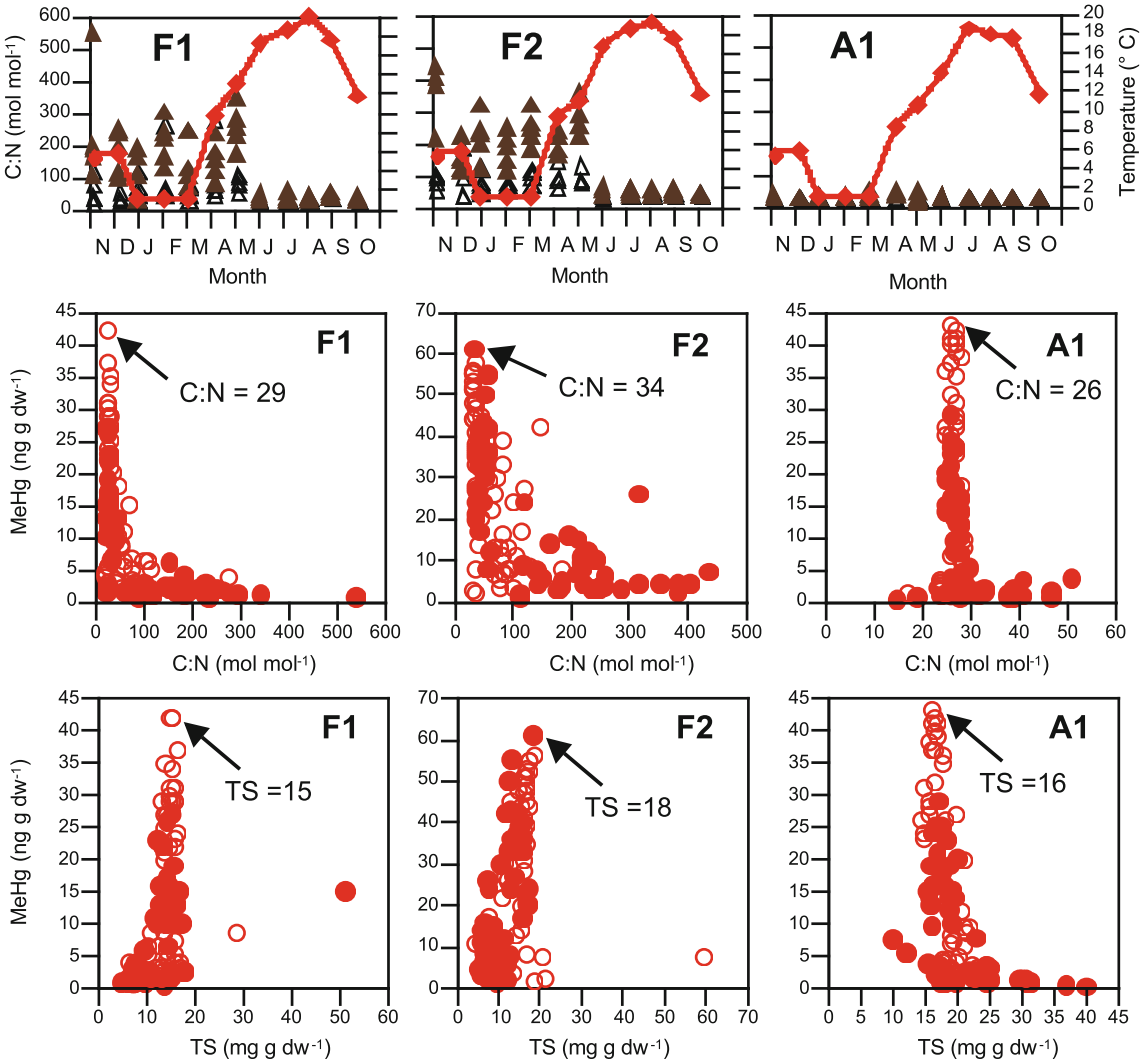

Fig. 5 *Upper panels* temporal change in C:N ratio in the 0–1 cm sediment layer (*open symbols*) and in the 1–5 cm sediment layer (*solid symbols*) at F1 (fiber sediment), F2 (fiber sediment), and A1 (nearby accumulation site) during the study period November 6, 2003–October 6, 2004. *Drawn curves* show temperature at the sediment–water interface. *Mid panels* MeHg plotted against C:N ratio for all samples from the 0 to 1 cm layers (*open symbols*) and from the 1 to 5 cm layers (*solid symbols*). The C:N ratio of the sample having the highest MeHg level is shown. *Lowest panels* MeHg plotted against total S (TS). A few samples are not included because the TS values were off scale. The TS level of the sample having the highest MeHg level is shown

sites at which accumulation of fine-particulate matter should be small. If settling matter did affect the profiles, fiber decomposition may have occurred in an even narrower band than suggested by the depth in the sediment (approximately 30 cm) at which the change in chemical composition started.

Until the May sampling, pockets of highly decomposed fibers remaining from earlier periods of decomposition were surrounded by fibers of variable decomposition state, as evidenced by the large variation in C:N ratios displayed by replicate sediment samples taken at F1 and F2, respectively. Subsequent mineralization resulted in more homogenous surface sediment consisting of highly decomposed fibers, as evidenced by the replicate sediment samples showing consistently low C:N ratios (Fig. 5). Evidently, the absence of strong winds allowed the decomposed fibers to stay in place during the summer–fall period.

At A1, the C:N ratios were low during the entire study in both the 0–1 cm and the 1–5 cm layers, and averaged 28 (Fig. 5). If autochtonous OM (algae) had made up most of the settling matter, the C:N ratio would have been closer to the Redfield ratio of ≈ 7. In the long core from A1, the C:N ratio was relatively stable down to approximately 0.5 m, suggesting that matter settling at A1 has been composed mainly of degraded fiber material since several decades back, and that postdepositional mineralization of this matter has been very slow (Fig. 2). Increasing THg toward

© Royal Swedish Academy of Sciences 2014

Table 2 Partial correlation coefficients ($r_{x\text{-}t}$) for logMeHg versus log(indicated variable) when *t* (time) was held constant. *T* (temperature) above the sediment surface was not log-transformed. All individual samples except identified outliers were included in the calculations

Sediment	TP	TS	TFe	TC	LOI	TFe:TS	TN	T	THg
F1 0–1 cm	0.49*	0.61*	0.23	−0.33*	−0.34*	−0.05	0.56*	0.40*	0.10
F1 1–5 cm	0.59*	0.63*	0.36*	−0.58*	−0.45*	0.12	0.58*	0.32*	−0.06
F2 0–1 cm	0.13	0.21	−0.02	−0.06	−0.03	−0.18	0.25	0.27*	0.57*
F2 1–5 cm	0.45*	0.46*	0.23	−0.31*	−0.40*	−0.09	0.55*	0.32*	0.18
A1 0–1 cm	0.06	−0.54*	−0.52*	0.82*	0.85*	−0.13	0.06	0.39*	0.49*
A1 1–5 cm	0.29*	−0.45*	−0.12	0.20	0.52*	0.64*	0.26	0.29*	0.32*

* $p < 0.05$

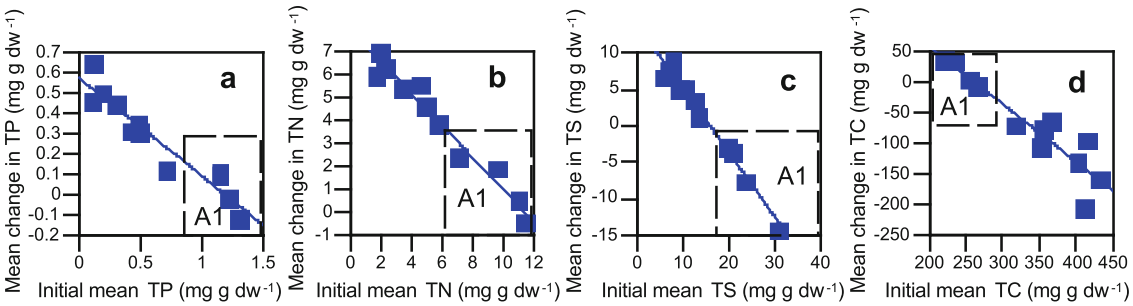

Fig. 6 Mean change in concentration between the dates May 6, 2004 and June 3, 2004 versus the mean concentration on May 6 (starting level), and, in the same plot, the mean change in concentration between the periods November 6, 2003–April 7, 2004 and July 8, 2004–October 6, 2004 versus the mean concentration for the period November 6, 2003–April 7, 2004 (starting level) for **a** total P, **b** total N, **c** total S, and **d** total C. For simplicity, all pair values are given the *same symbol* irrespective of layer (0–1 or 1–5 cm), station, and whether the value was generated from period or day values. *Boxes* separate the values of A1 from those of F1 and F2

the sediment–water interface could be a result of increasing THg in eroded material from the fiber sediment, and/or postdepositional upward movement of Hg.

It is important to know the factors controlling fiber decomposition not only because Hg methylation is linked to fiber decomposition, but also because the subsequent surface erosion of decomposed fibers could lead to the future exposure of aquatic organisms to higher contaminant levels. In Sweden, the use of Hg was banned in the mid 60s, suggesting that sub-surface peaks of Hg are present in fiber sediment. There may be sub-surface peaks also of other contaminants. A likely candidate is DDT (and its derivatives), because its use in forestry stopped in the mid 1970s. In both offshore and coastal sediment of the Baltic Sea, levels of DDT and its derivatives have been shown to increase with sediment depth (Jonsson et al. 2000).

It is clear that N and P uptake from water was required for efficient fiber decomposition. Dissolved oxygen levels should also be important, although sulfite pulp decomposition has been shown to proceed at significant rates also under anaerobic conditions as long as the level of nutrients is high (Hofsten and Edberg 1972). It is not clear, however, that N and P were limiting fiber decomposition in the sense that an increase in N and P availability should lead to increased rates of fiber decomposition, at least not in the 0–1 cm and 1–5 cm layers. In fact, the relationships shown in Fig. 6 suggest that available C in the fibers was limiting fiber decomposition, and needed to fuel microbial assimilation of N and P. It appears reasonable to state that nutrient availability as well as C quality determines the rate of fiber decomposition. Physical disturbance of sediment may lead to increased transfer of oxygen and nutrients to depths at which the organic C quality is high because of low previous exposure to microbial activity. It cannot be excluded that light contributed to fiber decomposition at the sediment–water interface, but we have no data supporting this notion.

An interesting question is how N was assimilated. Both cellulolytic *Clostridia* and SRB are known to fix N_2 (Fenchel and Finlay 1995; Bertics et al. 2010). If N_2 fixation explains most of the N-enrichment, P rather than N should be a limiting nutrient in fiber decomposition. Notably, TS correlated more strongly with TP than with TFe in most cases (Table 3). When P availability (or P uptake) is not an important factor in OM mineralization and SR, there would be little reason to expect TS to show as strong correlation with TP as with TFe. In fact, sulfide is known to cause release of P from Fe by forming $FeS_{(s)}$ (e.g., Olsson et al. 1997; Rozan et al. 2002).

© Royal Swedish Academy of Sciences 2014
www.kva.se/en

Hg Methylation in the Fiber Sediment

In natural sediment, the fraction of THg being MeHg is typically less than 1 % (Ullrich et al. 2001). In the fiber sediment of this study, the highest MeHg levels exceeded 3 % of THg, corresponding to absolute MeHg levels that were considerably higher than in unpolluted natural sediment.

Contrary to the C:N ratios (Fig. 5), the MeHg levels were similar in the replicate sediment samples until the May sampling and showed large variation thereafter (Fig. 4). In pockets of "old" decomposed fibers, MeHg levels may have been low because of demethylation and/or release of MeHg, potentially explaining both the low variation in MeHg before the June sampling and the high variation in MeHg levels at subsequent samplings that included both "old" decomposed and freshly decomposed fibers. Notably, if we had included winter months at the end of the study, we would likely have seen a decline in MeHg to pre-summer levels as a result of negative net methylation rates at lower temperatures (Ramlal et al. 1993).

Fiber decomposition leads to conditions conducive to Hg methylation, but Hg methylation was not a simple function of fiber decomposition. Hg methylation did not appear to show high rates until the C:N ratio had dropped to 30 mol mol^{-1} (Fig. 5), suggesting that electron donors suitable for microorganisms causing Hg methylation were lacking at higher C:N ratios. The microbial flora capable of Hg methylation may have been more diverse at F2 than at F1, because high MeHg levels were found over a broader range of C:N ratios at F2. Different time passed since the C:N ratios reached values optimal for MeHg could at least partly explain the high variation of MeHg at these C:N ratios (see previous discussion). Neither was there a simple relationship between Hg methylation and SR, because MeHg increased with TS only until a certain TS level was reached and then decreased (Fig. 5). SRB produce sulfide, resulting in increased retention of S, and are also known to methylate Hg, potentially explaining a positive relationship between MeHg and TS. The decrease in MeHg when TS increased above a certain level can be explained both by Hg becoming less available for methylation at higher sulfide levels and by losses of MeHg as a result of formation of water soluble MeHgSH (Skyllberg 2008).

Overall, TN was the sediment constituent showing the strongest correlation with MeHg (Tables 1, 2). Because N assimilation, P assimilation, C mineralization, and SR are interdependent processes, it is difficult and perhaps not even meaningful to single out any of them as the most critical process in Hg methylation. Microbial activity is temperature dependent, and temperature was certainly important (Table 2). Temperature effects on demethylation of MeHg are probably less than on Hg methylation (Ramlal et al. 1993).

In some cases, THg did not seem to have a significant effect on MeHg levels in the surface sediment (Table 2). However, when logTC or logTP accompanied logTHg in multiple regressions, logTHg became a significant predictor ($p < 0.05$) of logMeHg in all cases, suggesting that more MeHg would be formed if THg increased in the upper fiber sediment layers. In all cases, logMeHg increased significantly with logTN, logTP, and logTS, respectively, and decreased significantly with increasing logTC, but logTHg was not a significant variable in some of these regressions. The relationships were always markedly stronger for the 1–5 cm layers than for the 0–1 cm layers, possibly because the samples from the latter were more affected by settling matter and by disturbance caused by sampling (data not shown).

Table 3 Correlation coefficients (r) for indicated two-variable relationships. All individual samples including identified outliers were used in the calculations. No outlier values were identified from site A1

Sediment	logTS vs. logFe	logTS vs. logTP	logTFe vs. logTP
F1 0–1 cm	0.76	0.88	0.79
F1 1–5 cm	0.83	0.83	0.90
F2 0–1 cm	0.58	0.94	0.63
F2 1–5 cm	0.85	0.97	0.89
A1 0–1 cm	0.02	0.59	−0.34
A1 1–5 cm	0.71	0.57	0.75

Hg Methylation at Site A1

At A1, the C:N ratios were stable and close to 30 mol mol^{-1}, a ratio at which no or very little further change in the C:N ratio occurred at F1 and F2. Evidently, almost all labile organic C had been spent before settling at A1. Yet, this material seemed to have fueled a MeHg production that was almost as high as at F1 and F2 (Figs. 4, 5).

The strong correlation between MeHg and the TFe:TS ratio in the 0–10 cm layer was a contrasting feature when comparing the long core from A1 with those from F1 and F2 (Table 1). A high presence of sulfide-reactive Fe in relation to sulfide could prevent release of MeHg from the solid phase by reducing the formation of water soluble MeHgSH (Skyllberg 2008). Organically bound S can contribute to the MeHg binding capacity of the sediment, but this did not seem to be the case at A1. The TS versus TFe regression line ($r^2 = 0.95$) passed close to origin (intercept at −0.01 mmol S g dw^{-1}) and the mean concentration of TS was 1.5 mmol g^{-1} dw, leaving little room for organically bound S. The slope was 1.4, suggesting that

© Royal Swedish Academy of Sciences 2014

S was in the form of both $FeS_{(s)}$ and $FeS_{2(s)}$. The range of TFe:TS was 0.68–0.99 mol mol^{-1}. At F1 and F2, the regression line intercepted at 0.17 and 0.12 mmol S g dw^{-1}, whereas the mean TS concentration was 0.4 mmol g dw^{-1} in both cases, leaving room for a significant fraction of TS being organically bound.

A multiple regression analysis indicated that logMeHg co-varied strongly with both logTC ($p < 0.001$) and log(TFe:TS) ($p < 0.0005$) in the 0–10 cm layer at A1 ($n = 10$). The multiple regression model logMeHg = 24.2logTC + 3.10log(TFe:TS) − 58 explained 94 % of the vertical variation in logMeHg (MeHg: ng g dw^{-1}, TC: mg g dw^{-1}, TFe:TS: g g^{-1}). (Without log transformation, TC ($p < 0.005$) and TFe/TS ($p < 0.0001$) explained 95 % of the vertical variation in MeHg.) Substituting TC for LOI also resulted in both variables (LOI and TFe:TS) being significant predictor variables (data not shown). That the vertical variation of TC (258–268 mg g dw^{-1}) and of LOI (48.7–52.5 % of dw) was slight implies that most of the variation in OM was explained by freshly produced OM to which Hg methylation was tightly coupled.

LogMeHg co-varied with log(TFe:TS) also in the 0–1 cm and the 1–5 cm layers at A1 in the temporal study. Although log(TFe:TS) by itself was not correlated with logMeHg in the 0–1 cm layer (Table 2), multiple regressions showed that logTC and log(TFe:TS) both contributed significantly ($p < 0.001$ and $p < 0.0001$, respectively) to the variation in logMeHg in both layers. The models were logMeHg = 10.6logTC + 2.8log(TFe:TS) − 24.8, and logMeHg = 4.5logTC + 6.3log(TFe:TS) − 9.9 for the 0–1 cm and the 1–5 cm layers, respectively. They explained 47 and 75 % of the variation in logMeHg. The lower degree of explanation of these models compared with the model for the 0–10 cm layer of the long core could be due to more variable refractory OM levels. (Not just the fractions of OM associated with MeHg varied.) Apparently, both retention and production of MeHg controlled the MeHg levels in the sediment at A1.

At F1 and F2, MeHg increased when TC decreased (OM mineralization) and TS increased (sulfate reduction). In contrast, there was a gain in TC and a loss of TS when MeHg increased at A1 (Tables 1, 2). At all sites, the highest increase in sediment MeHg occurred between the May and June sampling (Fig. 4). At A1 during this period, TS decreased (the two symbols showing the lowest values on the *y*-axis in Fig. 6c), while TC increased (the two symbols showing the highest values on the *y*-axis in Fig. 6d). Clearly, microbial activities different from those at F1 and F2 were at play at A1. A possibility worth exploring is that TC increased and TS decreased as a result of C-fixation (chemolithoautotrophy) coupled to sulfide oxidation (e.g., Handley et al. 2013), the latter causing oxidative mobilization of S. Furthermore, syntrophic sulfur oxidation/reduction activity, in which sulfur oxidation regenerates oxidized S and fixes C to the benefit of Hg methylating SRB, could explain the MeHg production at A1.

The buried MeHg peak was a striking feature of the long sediment core from A1. It coincided with local maxima of TS, TP, TFe, and TC (Fig. 2). Possibly, the buried TS peak was a result of increased SR in conjunction with intrusion of brackish water, and/or in conjunction with increased P loads. The MeHg peak could be explained by active Hg methylation or by preservation of MeHg previously formed. The relatively low TFe:TS ratio of 0.72 mol mol^{-1} suggests that MeHg was not strongly retained at the depth of the buried MeHg peak, speaking in favor of active Hg methylation. The coincidence of elevated MeHg, TS, and TC levels fits the hypothesis that syntrophic sulfur oxidation/reduction is involved in Hg methylation at A1: While sulfur oxidation regenerates oxidized S and supplies fixed C to the benefit of SRB, SRB methylate Hg, generates CO_2 and replenish reduced sulfur. An absence of dissolved oxygen and nitrate does not preclude such a scenario, because fumarate produced by SRB could function as an electron acceptor when sulfide is oxidized (Woyke et al. 2006). There are other forms of syntrophy that could explain the buried MeHg peak. It has been demonstrated that a sulfate reducer, an incomplete oxidizer, and vigorous Hg methylator, could grow fermentatively in the absence of sulfate, using a methanogen as a sink for H_2 and acetate (Pak and Bartha 1998). Also, chemolithoautotrophy is represented among methane-forming archaea that use the reductive acetyl-coenzyme A pathway to fix CO_2 (Berg et al. 2010).

Final Remarks

Cellulose fiber sediments at different sites have different properties. Our study underscores the importance of characterizing cellulose fiber sediments with respect to major element composition in order to assess their present and future role as sources of bioavailable Hg. Also, risks associated with physical disturbance and high nutrient loads should be considered. Ideally, pore water studies should be included to be able to assess the extent to which MeHg and other contaminants leak out to the overlying water (Fathi et al. 2013). We believe there is reason for concern that contaminants (not just Hg) buried below layers of less contaminated cellulose fiber will become increasingly bioavailable as a result of fiber decomposition in the surface layers and subsequent erosion of decomposed fibers. Notably, different sites should be investigated and judged individually before any actions are taken to reduce future risks.

© Royal Swedish Academy of Sciences 2014
www.kva.se/en

Acknowledgments This study was part of a project initiated and run by the Kalmar County Administration and financed by the Swedish EPA. We thank the project manager Anna Aleljung and also Tommy Hammar, Kalmar County Administration and Bo Troedsson, Eman Catchment Management Association for taking part in the planning of the project and for providing equipment for field measurement and field sampling. As always, the mercury laboratory at IVL, Gothenburg determined mercury and methyl mercury with high accuracy and precision.

REFERENCES

Benoit, J.M., C.C. Gilmour, R.P. Mason, G.S. Riedel, and G.F. Riedel. 1998. Behavior of mercury in the Patuxent River estuary. *Biogeochemistry* 40: 249–265. doi:10.1023/A:1005905700864.

Berg, I.A., D. Kockelkorn, W.H. Ramos-Vera, R.F. Say, J. Zarzycki, M. Hügler, B.E. Alber, and G. Fuchs. 2010. Autotrophic carbon fixation in archaea. *Nature Reviews/Microbiology* 8: 447–460. doi:10.1038/nrmicro2365.

Bertics, V.J., J.A. Sohm, T. Treude, C.-E.T. Chow, D.G. Capone, J.A. Fuhrman, and W. Ziebis. 2010. Burrowing deeper into benthic nitrogen cycling: The impact of bioturbation on nitrogen fixation coupled to sulfate reduction. *Marine Ecology Progress Series* 409: 1–15. doi:10.3354/meps08639.

Bloom, N.S. 1992. On the chemical form of mercury in edible fish and marine invertebrate tissue. *Canadian Journal of Fisheries and Aquatic Sciences* 49: 1010–1017. doi:10.1139/f92-113.

Cleveland, C.C., and D. Liptzin. 2007. C:N: P stoichiometry in soil: Is there a "Redfield ratio" for the microbial biomass? *Biogeochemistry* 85: 235–252. doi:10.1007/s10533-007-9132-0.

Compeau, G.C., and R. Bartha. 1985. Sulfate-reducing bacteria: Principal methylators of mercury in anoxic estuarine sediment. *Applied and Environmental Microbiology* 50: 498–502.

Elser, J.J., W.F. Fagan, R.F. Denno, D.R. Dobberfuhl, A. Folarin, A. Huberty, S. Interlandl, S.S. Kilham, et al. 2000. Nutritional constraints in terrestrial and freshwater food webs. *Nature* 408: 578–580. doi:10.1038/35046058.

Fathi, M., J.J. Ridal, D.R.S. Lean, and J.M. Blais. 2013. Do wood fibers from pulp mill affect the distribution of total and methyl mercury in river sediments? *Journal of Great Lakes Research* 39: 66–73. doi:10.1016/j.jglr.2012.12.018.

Fenchel, T., and B.J. Finlay. 1995. *Ecology and evolution in anoxic worlds*. New York: Oxford University Press.

Fleming, E.J., E.E. Mack, P.G. Green, and D.C. Nelson. 2006. Mercury methylation from unexpected sources: Molybdate-inhibited freshwater sediments and an iron-reducing bacterium. *Applied and Environmental Microbiology* 72: 457–464. doi:10.1128/AEM.72.1.457-464.2006.

Fontaine, S., S. Barot, P. Barré, N. Bdioui, B. Mary, and C. Rumpel. 2007. Stability of organic carbon in deep soil layers controlled by fresh carbon supply. *Nature* 450: 277–280. doi:10.1038/nature06275.

Gavis, J., and J.F. Ferguson. 1972. The cycling of mercury through the environment. *Water Research* 6: 989–1008.

Handley, K.M., N.C. VerBerkmoes, C.I. Steefel, K.H. Williams, I. Sharon, C.S. Miller, K.R. Frischkorn, K. Chourey, et al. 2013. Biostimulation induces syntrophic interactions that impact C, S and N cycling in a sediment microbial community. *The ISME Journal* 7: 800–816. doi:10.1038/ismej.2012.148.

Hofsten, B.v., and N. Edberg. 1972. Estimating the rate of degradation of cellulose fibers in water. *Oikos* 23: 29–34.

Hultgren, P. 2000. Maringeologisk undersökning av Nötöfjärden, Oskarshamns kommun. Department of Marine Geology. Göteborg University (in Swedish).

Jonsson, P., J. Eckhéll, and P. Larsson. 2000. PCB and DDT in laminated sediments from offshore and archipelago areas of the NW Baltic Sea. *AMBIO* 29: 268–276. doi:10.1579/044-7447-29.4.268.

Naturvårdsverket. 1995. Branschkartläggningen: en översiktlig kartläggning av efterbehandlingsbehovet i Sverige. Rapport 4393. Naturvårdsverkets förlag. ISBN 91-620-4393-5 (in Swedish).

Olsson, S., J. Regnéll, A. Persson, and P. Sandgren. 1997. Sediment-chemistry response to land-use change and pollutant loading in a hypertrophic lake, southern Sweden. *Journal of Paleolimnology* 17: 275–294. doi:10.1023/A:1007967832177.

Pan-Hou, H.S., and N. Imura. 1982. Involvement of mercury methylation in microbial mercury detoxification. *Archives of Microbiology* 131: 176–177.

Pak, K.-R., and R. Bartha. 1998. Mercury methylation by interspecies hydrogen and acetate transfer between sulfidogens and methanogens. *Applied and Environmental Microbiology* 64: 1987–1990.

Parks, J.M., A. Johs, M. Podar, R. Bridou, R.A. Hurt, S.D. Smith, S.J. Tomanicek, Y. Qian, et al. 2013. The genetic basis for bacterial mercury methylation. *Science* 339: 1332–1335. doi:10.1126/science.1230667.

Ramlal, P.S., C.A. Kelly, J.W.M. Rudd, and A. Furutani. 1993. Sites of methyl mercury production in remote Canadian Shield lakes. *Canadian Journal of Fisheries and Aquatic Sciences* 50: 972–979. doi:10.1139/f93-112.

Regnell, O., and T. Hammar. 2004. Coupling of methyl and total mercury in a minerotrophic peat bog in southeastern Sweden. *Canadian Journal of Fisheries and Aquatic Sciences* 61: 2014–2023. doi:10.1139/F04-143.

Rozan, T.F., M. Taillefert, R.E. Trouwborst, B.T. Glazer, S. Ma, J. Herszage, L.M. Valdes, K.S. Price, et al. 2002. Iron–sulfur–phosphorus cycling in the sediment of a shallow coastal bay: Implications for sediment nutrient release and benthic macroalgal blooms. *Limnology and Oceanography* 47: 1346–1354. doi:10.4319/lo.2002.47.5.1346.

Skyllberg, U. 2008. Competition among thiols and inorganic sulfides and polysulfides for Hg and MeHg in wetlands soils and sediments under suboxic conditions: Illumination of controversies and implications for MeHg net production. *Journal of Geophysical Research* 113: G00C03. doi:10.1029/2008JG000745.

Sunderland, E.M., and G.L. Chmura. 2000. An inventory of historical mercury emissions in Maritime Canada: Implications for present and future contamination. *The Science of the Total Environment* 256: 39–57. doi:10.10167S0048-9697(00)00468-X.

Travnikov, O., I. Ilyin, O. Rozovskaya, M. Varygina, W. Aas, H.T. Uggerud, K. Mareckova, and R. Wankmueller. 2012. Long-term changes of heavy metal transboundary pollution of the environment (1990–2010). EMEP contribution to the revision of the heavy metal protocol. EMEP Status Report 2/2012.

Ullrich, S.M., T.W. Tanton, and S.A. Abdrashitova. 2001. Mercury in the environment: A review of factors affecting methylation. *Critical Reviews in Environmental Science and Technology* 31: 241–293. doi:10.1080/20016491089226.

Watras, C.J., and N.S. Bloom. 1992. Mercury and methylmercury in individual zooplankton: Implications for bioaccumulation. *Limnology and Oceanography* 37: 1313–1318. doi:10.4319/lo.1992.37.6.1313.

Woyke, T., H. Teeling, N.N. Ivanova, M. Huntemann, M. Richter, F.O. Gloeckner, D. Boffelli, I.J. Anderson, et al. 2006. Symbiosis insights through metagenomic analysis of a microbial consortium. *Nature* 443: 950–955. doi:10.1038/nature05192.

Yu, R.-Q., J.R. Reinfelder, M.E. Hines, and T. Barkay. 2013. Mercury methylation by the methanogen *Methanospirillum hungatei*. *Applied and Environmental Microbiology* 79: 6325–6330. doi:10.1128/AEM.01556-13.

© Royal Swedish Academy of Sciences 2014

Olof Regnell (✉), PhD, working at the Biological Department/ Aquatic Ecology, University of Lund, has studied the biogeochemistry of mercury in the aquatic environment since the late 80s. He has been expert advisor on mercury biogeochemistry, designed sampling programs, and evaluated field data in projects concerned with mercury-contaminated sites. His work demonstrates that combining environmental science and consultant work benefits both disciplines.
Address: Department of Biology, Aquatic Ecology, University of Lund, Sölvegatan 37, 223 62 Lund, Sweden.
e-mail: olof.regnell@biol.lu.se

Mark Elert, BSc, works as senior consultant at Kemakta Consultants. He has long experience of risk assessment of contaminated sediments and has been involved in a large number of sediment remediation projects in Sweden. His main expertise is modeling of contaminant release from sediments and their subsequent transport in lakes and rivers. Mark has been commissioned by Swedish environmental authorities to develop guidelines for various contaminants.
Address: Kemakta Konsult AB, Box 12655, 112 93 Stockholm, Sweden.
e-mail: mark@kemakta.se

Lars Olof Höglund, MSc, works as senior consultant at Kemakta Consultants. His field of expertise is close to that of Mark's and he, too, has been involved in a large number of sediment remediation projects in Sweden. His main expertise is modeling of chemical speciation and transformation of mercury and other contaminants in sediments and lakes. Lars Olof has been involved in several research projects funded by the Swedish Environmental Protection Agency and the Swedish Agency for Marine and Water Management.
Address: Kemakta Konsult AB, Box 12655, 112 93 Stockholm, Sweden.
e-mail: loh@kemakta.se

Anna Helena Falk, MSc, works as a consultant at Akvaplan-niva, Norway. Her main responsibilities are investigations and monitoring of polluted areas and environmental risk analysis. She has been studying both organic pollutants and heavy metals.
Address: Akvaplan-niva AS, FRAM - High North Research Centre for Climate and the Environment, 9296 Tromsö, Norway.
e-mail: ahf@akvaplan.niva.no

Anders Svensson, BSc, works at the Kalmar County administration board. State financed remediation projects and water quality monitoring of hazardous substances are his main duties.
Address: Environmental Unit, Kalmar County Administration, 391 86 Kalmar, Sweden.
e-mail: anders.svensson@lansstyrelsen.se

© Royal Swedish Academy of Sciences 2014
www.kva.se/en